(*Abstract for the 36th International Workshop on Water Waves and Floating Bodies, Seoul, Korea, 2021*)

# Phase Locking Phenomenon in the Modulational Instability of Surface Gravity Waves

Shuai Liu[1]*, Takuji Waseda[2], Xinshu Zhang[1]†

[1] State Key Laboratory of Ocean Engineering, Shanghai Jiao Tong University, Shanghai 200240, China

[2] Graduate School of Frontier Sciences, University of Tokyo, Kashiwa, Chiba 277-8563, Japan

## 1 Introduction

Freak wave (also called rogue wave or extreme wave) is an anomalous, short-term wave that is much higher than expected for the sea state. Over the past thirty years, the freak wave has attracted considerable attention, and several different mechanisms have been found to be responsible for its generation (see the general reviews in Dysthe *et al.*, 2008; Onorato *et al.*, 2013). In absence of specific environmental forcing, one possible mechanism is energy focusing introduced by second-order nonlinearity. On the other hand, the modulational instability, (also called Benjamin-Feir instability, Benjamin & Feir, 1967) enhanced by third-order nonlinearity also plays a significant role, especially for deep-water long-crested waves (Tang *et al.*, 2021).

The modulational instability of a plane wave to perturbation sidebands is a kind of four-wave quasi-resonant interactions

$$2\vec{k_1} - \vec{k_3} - \vec{k_4} = 0, \quad 2\omega_1 - \omega_3 - \omega_4 = O(\varepsilon^2), \tag{1}$$

where $\vec{k_i}$ are the wavenumbers, $\omega_i$ are the angular frequencies and $\varepsilon$ is the wave steepness. Considering a plane wave $\vec{k_1}$ with two perturbation sidebands $\vec{k_3} = \vec{k_1} - \vec{k}$ and $\vec{k_4} = \vec{k_1} + \vec{k}$ ($\vec{k}$ is the perturbation wavenumber), the energy is transferred between different components through four-wave quasi-resonance. This process can be well described by the Zarkharov's equation (ZE) or the nonlinear Schrödinger equation (NLSE). The amplitudes of two perturbations were found to grow exponentially at the expense of the plane wave. As a result, large waves are likely to be formed due to the strong nonlinear focusing. Over the past decades, the evolution of wave amplitude has been investigated theoretically, numerically, and experimentally (e.g. Waseda & Tulin, 1999; Ma *et al.*, 2012). In contrast, the phase evolution of each wave due to the modulational instability has received less attention.

Here, we study the modulational instability through ZE and a higher-order spectral (HOS) method. Particular attention is paid to the phase evolution. The results of ZE with the support of HOS simulations show a phase locking phenomenon in the modulational instability. To the authors' knowledge, it is the first time to show this feature of modulational instability.

## 2 Theoretical analyses

The four-wave reduced equation for pure gravity waves from ZE reads (Zakharov, 1968)

$$\mathrm{i}\partial_t B_1 = \int T_{1234} B_2^* B_3 B_4 \delta_{1+2-3-4} \exp\left(\mathrm{i}\Delta_{1234} t\right) \mathrm{d}\boldsymbol{k}_{2,3,4}, \tag{2}$$

where $B_i$ is the wave action amplitude and its relation to wave amplitude is $a_i = \sqrt{2\omega_i/g}|B_i|$. Considering the stability of wave $\vec{k_1}$ with two collinear disturbances at $\vec{k_3} = \vec{k_1} + \vec{k}$ and $\vec{k_4} = \vec{k_1} - \vec{k}$, the evolution equations are obtained as follow

$$\begin{aligned}
\mathrm{i}\partial_t B_1 &= \left(\Omega_1 - \omega_1\right) B_1 + 2T_{1134} \exp(\mathrm{i}\Delta_{1134} t) B_1^* B_3 B_4, &(3)\\
\mathrm{i}\partial_t B_3 &= \left(\Omega_3 - \omega_3\right) B_3 + T_{1134} \exp(-\mathrm{i}\Delta_{1134} t) B_1^2 B_4^*, &(4)\\
\mathrm{i}\partial_t B_4 &= \left(\Omega_4 - \omega_4\right) B_4 + T_{1134} \exp(-\mathrm{i}\Delta_{1134} t) B_1^2 B_3^*, &(5)
\end{aligned}$$

and

$$\begin{aligned}
\Omega_1 &= \omega_1 + T_{1111}\left|B_1\right|^2 + 2T_{1313}\left|B_3\right|^2 + 2T_{1414}\left|B_4\right|^2, &(6)\\
\Omega_3 &= \omega_3 + 2T_{1313}\left|B_1\right|^2 + T_{3333}\left|B_3\right|^2 + 2T_{3434}\left|B_4\right|^2, &(7)\\
\Omega_4 &= \omega_4 + 2T_{1414}\left|B_1\right|^2 + 2T_{3434}\left|B_3\right|^2 + T_{4444}\left|B_4\right|^2, &(8)
\end{aligned}$$

*Presenting author

†xinshuz@sjtu.edu.cn

where $\Delta_{1134} = 2\omega_1 - \omega_3 - \omega_4$ is the detuning factor, $\Omega_i$ are the nonlinear frequencies and $T$ represents the interaction kernel.

Assuming the amplitudes of sidebands are much smaller than that of plane wave $|B_3|, |B_4| \ll |B_1|$, the evolution equations are reduced to

$$\mathrm{i}\partial_t B_1 = T_{1111}\left|B_1\right|^2 B_1, \tag{9}$$

$$\mathrm{i}\partial_t B_3 = 2T_{1313}\left|B_1\right|^2 B_3 + T_{1134}e^{\mathrm{i}-\Delta_{1134}t}B_1^2 B_4^*, \tag{10}$$

$$\mathrm{i}\partial_t B_4 = 2T_{1414}\left|B_1\right|^2 B_4 + T_{1134}e^{\mathrm{i}-\Delta_{1134}t}B_1^2 B_3^*. \tag{11}$$

The solution of $B_1$ is obatained from equation (9) as

$$B_1 = \beta_1 e^{-\mathrm{i}T_{1111}\beta_1^2 t}, \quad \beta_1 = B_1(0), \tag{12}$$

To solve equations (10) and (11), Mei *et al.* (2005) made an assumption that the solutions follow the following expressions

$$B_3 = \beta_3 e^{-\mathrm{i}\left[\frac{1}{2}\Delta_{1134}+T_{1111}\beta_1^2+\sigma\right]t}, \quad \beta_3 = B_3(0), \tag{13}$$

$$B_4 = \beta_4 e^{-\mathrm{i}\left[\frac{1}{2}\Delta_{1134}+T_{1111}\beta_1^2-\sigma^*\right]t}, \quad \beta_4 = B_4(0). \tag{14}$$

The eigenvalue $\sigma$ is given by

$$\sigma = \left(T_{1313} - T_{1414}\right)\beta_1^2 \pm D^{1/2}, \tag{15}$$

where

$$D = \left[\frac{1}{2}\Delta_{1134} + \left(T_{1111} - T_{1313} - T_{1414}\right)\beta_1^2\right]^2 - T_{1134}^2\beta_1^4. \tag{16}$$

If the value of $D$ is positive, the modulus of $B_3$ and $B_4$ is stable with time. But, if $D$ is negative, $B_3$ and $B_4$ tends to increase exponentially with time. The value of growth rate is given by the imaginary part of $\sigma$, i.e., $\mathrm{Im}[D^{1/2}]$.

Besides, from equations (12), (13) and (14), the phases of the plane wave and two sidebands are given by

$$\varphi_1 = -T_{1111}\beta_1^2 t + \varphi_1(0), \tag{17}$$

$$\varphi_3 = -\left[\frac{1}{2}\Delta_{1134} + T_{1111}\beta_1^2 + \mathrm{Re}[\sigma]\right]t + \varphi_3(0), \tag{18}$$

$$\varphi_4 = -\left[\frac{1}{2}\Delta_{1134} + T_{1111}\beta_1^2 - \mathrm{Re}[\sigma^*]\right]t + \varphi_4(0). \tag{19}$$

The individual phase of each wave is supposed to change linearly with time, and the interaction phase follows

$$\varphi = 2\varphi_1 - \varphi_3 - \varphi_4 = 2\varphi_1(0) - \varphi_3(0) - \varphi_4(0) + \Delta_{1134}t. \tag{20}$$

Considering the detuning factor is $\Delta_{1134} \sim O(\varepsilon^2)$, the value of $\Delta_{1134}t$ is almost negligible in the initial stage. Thus, the interaction phase is expected to be locked at $\varphi = \varphi(0)$.

However, these results of wave amplitude and phase are limited to the assumption of the expression of $B_3$ and $B_4$. To overcome this, we directly solve the differential equations (10) and (11) by the 4th-order Runge-Kutta method. Both of these direct numerical results (ZE-NUM) and the results from the analytical expressions (ZE-ANA) are reported in the present paper.

# 3 Phase-resolved numerical simulations

We also conducted numerical simulations of modulated wave groups by the HOS method (Dommermuth & Yue, 1987; West *et al.*, 1987). This phase-resolved method directly solves the Euler equation with the nonlinear surface boundary conditions in Zakharov's form. HOS method has been widely applied in wave modelling (e.g. Liu & Zhang, 2019). To improve the computing efficiency, we developed HOS method in house combined with a GPU-accelerated computing technique.

The imposed modulated wave group is as follows

$$\eta = a_1\cos(k_1 x + \varphi_1(0)) + a_3\cos(k_3 x + \varphi_3(0)) + a_4\cos(k_4 x + \varphi_4(0)). \tag{21}$$

We considered a typical case, a plane wave with $k_1 = 1$ and $a_1 = 0.12$ is modulated by a lower sideband at $k_3 = 1.20$ and a upper sideband at $k_4 = 0.80$, i.e. $\varepsilon = k_1 a_1 = 0.12$ and $k/k_1 = 0.20$. The amplitude ratio between the plane wave and sidebands is 0.01. The initial phase of perturbation sidebands is fixed at $\varphi_3(0) = \varphi_4(0) = -\pi/4$ where the maximum growth rate of sidebands is achieved (Benjamin & Feir, 1967).

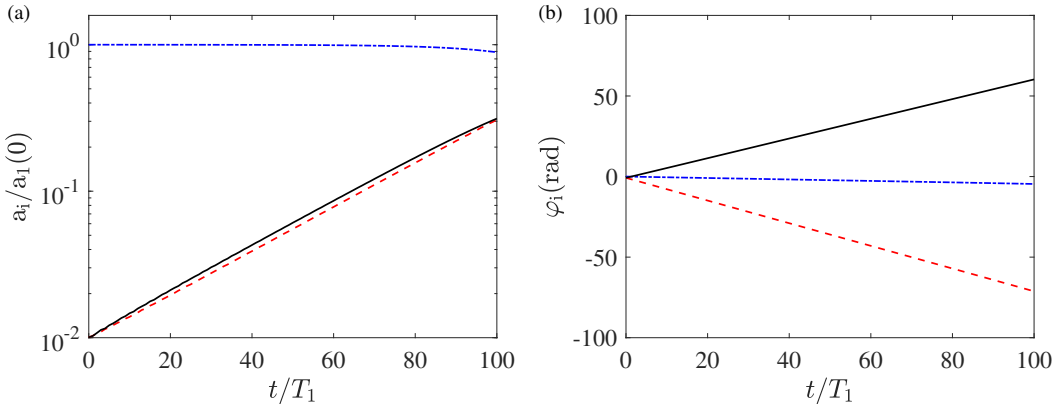


Figure 1: Temporal evolution of the amplitude (a) and phase (b) of each wave from HOS simluations. The wave amplitudes are normalized by the initial amplitude of plane wave $a_1(0)$. $i = 1(-\cdot-)$, $3(- - -)$, $4(——)$.

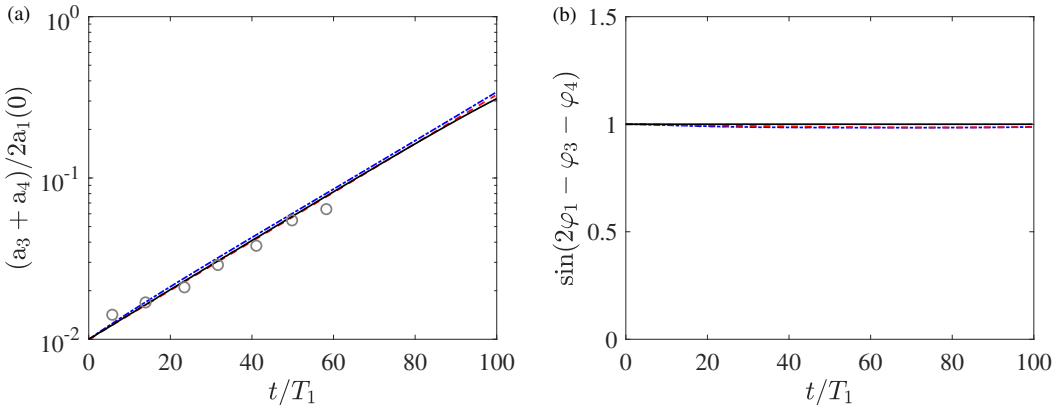


Figure 2: (a) Temporal evolution of the normalized mean amplitude $(a_3 + a_4)/2a_1(0)$ (b) temporal evolution of the sine of interaction phase $\varphi = 2\varphi_1 - \varphi_3 - \varphi_4$. The initial phases are $\varphi_3(0) = \varphi_4(0) = -\pi/4$. The experimental results from Tulin & Waseda (1999) are also shown in panel (a) by the circulars. HOS$(-\cdot-)$, ZE-NUM$(- - -)$, ZE-ANA$(——)$.

The evolutions of this modulated wave group over deep water depth are simulated in a one-dimensional domain of $10\lambda_1$ length with periodic boundary conditions ($\lambda_1 = 6.28$m is the wave length corresponding to $k_1 = 1$). We have to remark that the resolution in wavenumber domain depends on the length of computation domain. Here, we get the resolutions $\mathrm{d}k = 0.1$, which allows us to accurately extract the sidebands ($k_3 = 0.80$ and $k_4 = 1.20$). To focus on the effect of modulational instability, third-order expansion in the wave steepness of the velocity potential and the vertical velocity on the free surface (i.e. M=3) are included. 256 nodes are used to capture the surface elevation and velocity potential, namely, about 25 nodes for every wave length.

Figure 1(a) and (b) show the temporal evolutions of amplitude and phase of each wave, respectively. The wave amplitudes are normalized by the initial amplitude of plane wave $a_1(0)$, and the time $t$ is normalized by wave period of plane wave $T_1$. Results show the amplitudes of sidebands grow exponentially with time and the phases of each wave vary linearly. These results are in agreement with the predictions of ZE-ANA. The wave steepness is small during the simulations, so the exponential growth of wave amplitude and linearly variation of wave phase are still visible for longer times. Besides, the amplitude evolutions of upper sideband and lower sideband are in good consistent during the simulation.

To quantitatively compare the HOS results with ZE, figure 2 shows the temporal evolution of the normalized mean amplitude $(a_3 + a_4)/2a_1(0)$ and the sine of interaction phase $\varphi = 2\varphi_1 - \varphi_3 - \varphi_4$ from HOS, ZE-NUM and ZE-ANA. Experimental observations from Tulin & Waseda (1999) are also plotted in panel (a) for reference. They have been transferred from spatial domain to temporal domain based on the group velocity of the plane wave. The amplitude growths of sidebands from different methods are in good agreement with experimental results, which provide a direct validation of the present numerical simulations and analyses. The results for interaction phase from HOS, ZE-NUM and ZE-ANA are also in good agreement, and a clear phase locking phenomenon is observed.

We further changed the initial phase of sidebands to assess its effect on phase locking and amplitude growth of modulational instability. Apart from the above test case $\varphi_3(0) = -\pi/4$ and $\varphi_4(0) = -\pi/4$, the modulated wave groups with $\varphi_3(0) = \varphi_4(0) = 0, \pi/4$ and $\pi/2$ are modelled. The temporal evolution of mean amplitude $(a_3 + a_4)/2$ and interaction phase $2\varphi_1 - \varphi_3 - \varphi_4$ are presented in figure 3. As illustrated before, if

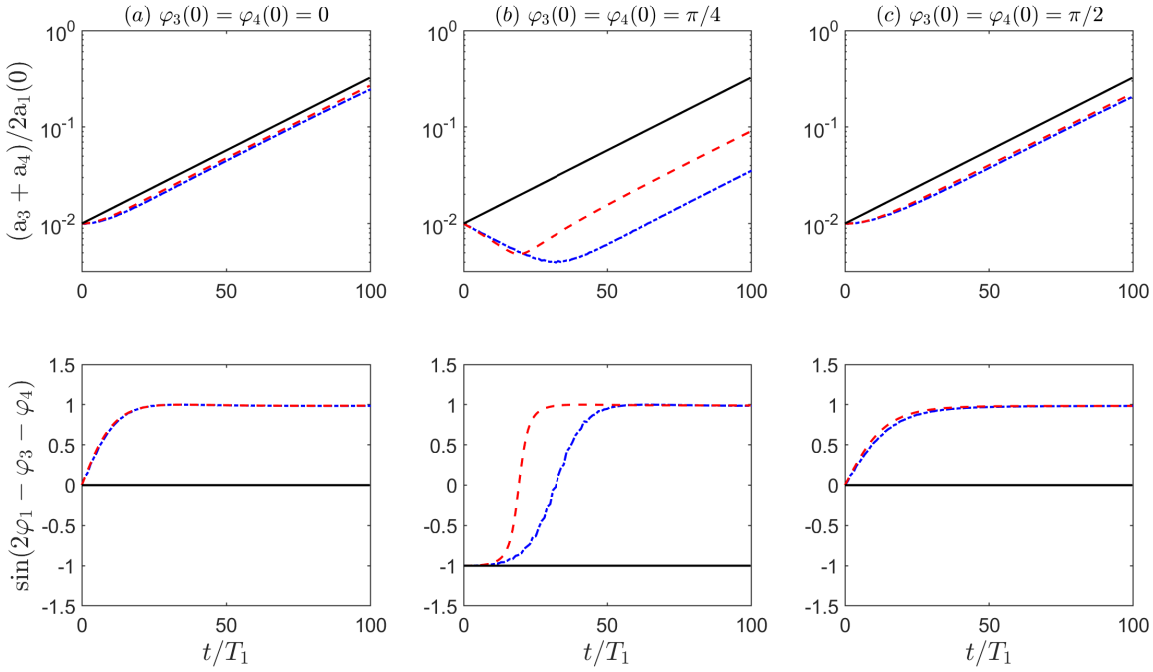


Figure 3: The temporal evolution of mean amplitude $(a_3 + a_4)/2a_1(0)$ and interaction phase $2\varphi_1 - \varphi_3 - \varphi_4$ with initial phase $\varphi_3(0) = \varphi_4(0) = 0$, $\pi/4$ and $\pi/2$. HOS($- \cdot -$), ZE-NUM($- - -$), ZE-ANA(——).

$\varphi_3(0) = \varphi_4(0) = -\pi/4$, the mean amplitude of sidebands increases exponentially with time and the interaction phase stays constant. However, when the initial phases $\varphi_3(0)$ and $\varphi_4(0)$ are not equal to $-\pi/4$, HOS results with the support of ZE-NUM show that, the interaction phase changes with time in the initial stage and then stay constant as it reaches $\varphi = \pi/2$. Meanwhile, the mean amplitude of perturbation sidebands changes non-exponentially with time for short times. Once the interaction phase increases to lock at $\varphi = \pi/2$, the amplitude tends to increase exponentially. Note that, for the case with $\varphi_3(0) = \varphi_4(0) = \pi/4$, the time of reaching steady in HOS are larger than in from ZE-NUM. Except for this the results of HOS and ZE-NUM are in excellent agreement. The results of ZE-ANA are not applicable here due to the assumption of form of solutions. Besides, for all the test cases, the exponential growth rates of the sidebands' amplitude are in good agreement, which suggests that the growth rate is independent on the initial phases of sidebands. More results will be presented in the workshop.

# References


Benjamin, T. B. & Feir, J. E. 1967 The disintegration of wave trains on deep water Part 1. Theory. *Journal of Fluid Mechanics* **27**, 417–430.

Dommermuth, D. & Yue, D. K. P. 1987 A higher-order spectral method for the study of nonlinear gravity waves. *Journal of Fluid Mechanics* **187**, 267–288.

Dysthe, Kristian, Krogstad, Harald E. & Muller, Peter 2008 Oceanic rogue waves. *Annual Review of Fluid Mechanics* **40** (1), 287–310.

Liu, S. & Zhang, X. S. 2019 Extreme wave crest distribution by direct numerical simulations of long-crested nonlinear wave fields. *Applied Ocean Research* **86**, 141–153.

Ma, Y., Dong, G., Perlin, M., Ma, X. & Wang, G. 2012 Experimental investigation on the evolution of the modulation instability with dissipation. *Journal of Fluid Mechanics* **711**, 101–121.

Mei, C. C., Stiassnie, M. & Yue, D. K. P. 2005 *Theory and Applications of Ocean Surface Waves, Part 2: Nonlinear Aspects*.

Onorato, M., Residori, S., Bortolozzo, U., Montina, A. & Arecchi, F. T. 2013 Rogue waves and their generating mechanisms in different physical contexts. *Physics Reports* **528** (2), 47–89.

Tang, Tianning, Xu, Wentao, Barratt, Dylan, Bingham, H. B., Li, Y., Taylor, P. H., van den Bremer, T. S. & Adcock, T. A. A. 2021 Spatial evolution of the kurtosis of steep unidirectional random wavesn. *Journal of Fluid Mechanics* **908** (A3).

Tulin, Marshall P. & Waseda, Takuji 1999 Laboratory observations of wave group evolution, including breaking effects. *Journal of Fluid Mechanics* **378**, 197–232.

Waseda, T. & Tulin, M. P. 1999 Experimental study of the stability of deep-water wave trains including wind effects. *Journal of Fluid Mechanics* **401**, 55–84.

West, B. J., Brueckner, K. A. & Janda, R. S. 1987 A new numerical method for surface hydrodynamics. *Journal of Geophysical Research* **92** (11), 11803–11824.

Zakharov, V. E. 1968 Stability of periodic waves of finite amplitude on the surface of a deep fluid. *Journal of Applied Mechanics & Technical Physics* **9** (2), 190–194.